ELSEVIER

Nuclear Instruments and Methods in Physics Research B 143 (1998) 357–370

NIM B
Beam Interactions with Materials & Atoms

$^{12}C(\alpha,\alpha)^{12}C$ resonant elastic scattering at 5.7 MeV as a tool for carbon quantification in silicon-based heterostructures

M. Berti [a,*], D. De Salvador [a], A.V. Drigo [a], F. Romanato [a,1], A. Sambo [a], S. Zerlauth [b], J. Stangl [b], F. Schäffler [b], G. Bauer [b]

[a] *INFM at the Physics Department, University of Padova, Via Marzolo 8, 35131 Padova, Italy*
[b] *Institute for Semiconductor Physics, Kepler University Linz, Altenbergerstr.69, A-4040 Linz, Austria*

Received 27 November 1997; received in revised form 24 April 1998

Abstract

The incorporation of carbon into substitutional sites in Si or $Si_{1-x}Ge_x$ attracts increasing interest due to the enhanced possibilities in strain and band gap engineering of group IV heterostructures. Precise and accurate measurement of carbon concentration is, however, quite difficult to achieve. We focused our attention on the study of the alpha resonant elastic scattering in the 5.7 MeV energy region. We measured the scattering cross-section in the range 5.4–6.0 MeV at a laboratory scattering angle of 170°. The results indicate that the cross-section value is enhanced with respect to the Rutherford one of an almost constant factor (×130) in an energy interval about 100 keV wide. This allows a more accurate measurement of carbon concentration than with the normally used 4.265 MeV resonance. The experimental procedure to deal with non-Rutherford scattering of Si has been also determined. The resonant scattering at 5.72 MeV has been used, in combination with Rutherford Backscattering Spectrometry (RBS) at 3.0 MeV, to determine the carbon content of three $Si_{1-x-y}Ge_xC_y$ samples. This has also been used, in channelling geometry, to determine the substitutional carbon fraction of the samples.

PACS: 61.18 Bn; 61.85 p; 61.10 i; 65.50
Keywords: Nuclear techniques; Carbon determination; SiGeC alloys

1. Introduction

Pseudomorphic $Si_{1-x}Ge_x$ layers are extensively studied due to the possibility of band gap tailoring. The energy gap, as well as the band structure and the band offset, are related to the composition and to the built in strain of the layer. Strong limitations to obtain thick pseudomorphic layers arise from the fact that when the equilibrium critical thickness is exceeded strain relief occurs leading to misfit dislocation formation, the equilibrium critical thickness being dependent on the strain in the layer. It has been shown that the addition in the

* Corresponding author. Tel.: 39 498277038; fax: 39 488277003; e-mail: berti@padova.infm.it.
[1] Present address: INFM-TASC at Elettra, S.S.14 Km 163.5, Area Science Park, 34012 Basovizza – Trieste, Italy.

0168-583X/98/$19.00
PII: S0168-583X(98)00323-1

alloy of small amounts of carbon as substitutional impurity can be used to decrease the lattice mismatch of the SiGe layer to the substrate and that a $Si_{1-x-y}Ge_xC_y$ alloy with $x = 0.200$ and $y = 0.018$ has an indirect band gap of 1.3–1.7 eV [1].

The Si lattice is about 50% greater than the diamond lattice ($a_{Si} = 0.5431$nm, $a_C = 0.3567$ nm) and 4% smaller than the Ge lattice, thus, by controlling the amount of the added carbon, it is possible to obtain an alloy with the Si lattice parameter and even alloys where tensile strain is produced [2]. However strong practical limitations to the addition of carbon in substitutional sites arise from its very low bulk solubility in Si ($\sim 3 \times 10^{17}$ at/cm^3 at the melting point [3]); carbon substitutional concentrations of a few at.% can be reached only by growth techniques far from thermodynamic equilibrium such as molecular beam epitaxy (MBE) or chemical vapour deposition (CVD). Besides the interest in studying the $Si_{1-x-y}Ge_xC_y$ pseudomorphic layers, renewed attention is now been paid to the $Si_{1-y}C_y$ alloys.

When both the above mentioned systems are under study the possibility of achieving an accurate quantification of the carbon content in the alloy is of crucial importance and at the same time very difficult. In particular, in the case of typical $Si_{1-x-y}Ge_xC_y$ layers, the carbon concentration is usually of the order of 1at.% and the thickness of the layers is limited to a few hundreds of nanometers or less. Hence the total amount of carbon involved (about 10^{16} at/cm^2) is comparable to the surface carbon contamination, unless very accurate cleaning procedures are used. Moreover the knowledge of the carbon concentration profile does not completely characterise $Si_{1-x-y}Ge_xC_y$ and $Si_{1-y}C_y$ layers. In fact, also the microstructure and the substitutional C fraction must be determined.

A variety of techniques have been used to characterise $Si_{1-x-y}Ge_xC_y$ or $Si_{1-y}C_y$ alloys, both from the compositional and from the structural point of view. In most cases two or more techniques are jointly used to achieve a complete characterisation of the layers. For example, by using Secondary Ion Mass Spectrometry (SIMS) one can measure very small carbon concentrations but no information about the structure of the samples is obtained. In these cases Transmission Electron Microscopy (TEM) is often used in combination [4–6]. Moreover quantitative calibration of the SIMS measurements is found to be difficult because of the lack of very accurate standard samples and of matrix effects [7].

In principle Ion Beam Analysis is a good tool to obtain compositional and structural (in channelling geometry) information. Among the ion beam techniques the otherwise employed $^{12}C(d,p)^{13}C$ nuclear reaction cannot be used to obtain depth concentration profiles of carbon in shallow layers close to the surface because of the poor depth resolution that does not allow to distinguish between carbon in the film and carbon in the surface contaminants. Helium Rutherford Backscattering Spectrometry (RBS) has a sufficient depth resolution but too poor sensitivity to detect carbon concentrations in the range of a few atomic percent in heavier matrices like Si and SiGe, due to the Z^2 dependence of the scattering cross-section. It is possible to overcome this difficulty by exploiting resonances in the elastic scattering cross-section occurring at relatively high beam energy.

The most used non-Rutherford elastic reaction is the resonant alpha scattering at 4.265 MeV. Its use for the analysis of carbon content in thin films was first suggested in Ref. [8]. The cross-section was measured for a scattering angle of 170° by Leavitt et al. [9] and for 165° by Feng et al. [10]. At the resonance maximum the cross-section value is about 130 times the Rutherford one and the resonance width (FWHM) is reported to be about 40 keV. The strong enhancement of the cross-section is clearly desirable when small amounts of carbon must be measured, nevertheless, as many of the researchers who used this reaction already stated [11,12], "its use requires a rather careful, time-consuming procedure to ensure C/Si ratios of reasonable accuracy". The main factors affecting the results are the rapid variation of the cross-section with the energy of the analysing beam together with the width of the resonance. In fact it is too large to allow depth profiling with the usual "resonance depth profiling" [13] but it is too narrow to allow the detection of C in the whole layer with constant cross-section. The energy of the α particles crossing the SiC layer must be known

with an accuracy better than ±5 keV otherwise large errors in the measured C areal density could occur. This means that the initial beam energy and the energy lost in the SiC layer (i.e. stopping power and film thickness) must be accurately checked before measuring. For this reason the technique is best suited to measure C/Si ratios in thick (some μm), uniform films but it looses accuracy when thin films with possible changes in composition are under study. The same holds true for the structural characterisation by channelling. The difference between the aligned (axial) and random stopping power causes the maximum of the cross-section to occur at different depths of the sample. This fact does not influence the results in a thick, uniform film whereas it could induce relevant errors in thin film analysis.

Another possible ion beam technique is Elastic Recoil Detection Analysis (ERDA) by using high energy heavy ions. In the case of Si–C alloys the commonly used Si beam does not allow to have any reference signal in the spectrum so that absolute calibration of the experiments is needed, which is a very difficult task. Moreover ERDA does not allow lattice location experiments.

Of course High Resolution X-Ray diffraction (HRXRD) is an excellent technique to measure the structural parameters of strained layers. However C concentration values from HRXRD data are based on the assumption that all the C is on substitutional sites and on the validity of Vegard's rule [14]. The Vegard's rule is known to be invalid for the SiGe system [15] and it certainly does not hold for the lattice parameters of Si, β-SiC and diamond. Moreover recent Raman results [16] suggest some discrepancy with the C concentration determined by the 4.265 MeV resonance. Finally a recent theoretical work [17] points to a substantial deviation from Vegard's rule over the whole Si–C composition range so that the former agreement between HRXRD data and C concentration and lattice location data obtained by the 4.265 MeV resonance (see e.g. Ref. [4]) must be questioned. The availability of another technique to measure C/Si ratios is thus desirable and is the aim of this paper.

In the framework of resonant backscattering, measuring C/Si ratios with good accuracy and performing C lattice location requires not only a strong enhancement of the elastic cross-section but also a constant value of the cross-section over a wide range of the beam energy.

Feng et al. [10] showed that in the energy interval from 5.0 to 6.0 MeV the $^{12}C(\alpha,\alpha)^{12}C$ cross-section, when measured at 165° in the laboratory frame, exhibits a very broad resonance peak centred at about 5.7 MeV where the enhancement factor with respect to the Rutherford cross-section value is about 120 times. Around the maximum the cross-section can be assumed to be constant within 4% of its value in an energy interval of about 150 keV. Therefore this broad resonance peak appears to be a good candidate for measuring small carbon quantities with good accuracy. The data of Ref. [10] were taken at a laboratory scattering angle of 165° and further measurements [18] suggest a significant dependence of the cross-section on the scattering angle. For this reason we first undertook a systematic measure of the ratio of the $^{12}C(\alpha,\alpha)^{12}C$ reaction cross-section with respect to the Rutherford one in the 5.4–6.0 MeV range and for a scattering angle of 170°. Further, as in this energy region the Si cross-section is also strongly non-Rutherford, the second objective of the present work was to find suitable measuring conditions to overcome this problem. Finally, to test the technique, the C concentration and lattice location of three SiGeC/Si samples were measured and compared to the results of HRXRD.

2. Experimental

The experiments have been performed at Laboratori Nazionali di Legnaro (LNL) by using $^4He^+$ beams delivered by the 7 MV CN Van de Graaff accelerator. The beam energy calibration was accurately performed some time ago by using narrow cross-section resonances and NMR magnetic field calibration. The present beam energy accuracy relies on the overall stability of the analysing magnet and NMR probe. In the present experiment, by using the $^{16}O(\alpha,\alpha)^{16}O$ and $^{12}C(\alpha,\alpha)^{12}C$ resonances at 3.054 and 4.265 MeV, respectively, we can estimate the beam energy uncertainty at 6 MeV to be no more than ±5 keV.

The scattering chamber is evacuated by a turbomolecular pump giving a vacuum in the 10^{-7} mbar range. At the chamber entrance different diaphragms can be selected so that the beam spot on the sample can be changed both in shape and size. Two solid state Si detectors can be independently and remotely moved by stepping motors to any angle in the range 0–180°. The differential precision in the angle setting is better than 0.01° while the absolute value of the angle can be calibrated within each run with respect to the actual beam direction with a precision better than 0.05°. This fact is very important in the case of grazing angle incidence and/or emergence experiments.

Two different sample manipulators can be used. For very precise channelling measurements a home-made 3-axis goniometer is used. The main tilt axis ($\hat{\vartheta}_x$) allows ±90° rotation while the $\hat{\vartheta}_y$ axis is limited to ±30°. The azimuthal axis ($\hat{\vartheta}_z$) allows 360° rotation. All the rotations have both precision and repeatability of 0.01°. An X–Y table allows to change the beam spot position on the sample surface over ±16 mm in both directions while maintaining the beam at the common crossing of the 3-rotation axes.

A second sample holder allows to mount up to 40 samples 1×1 cm^2 and has two tilt rotation axes ($\hat{\vartheta}_x$ and $\hat{\vartheta}_y$), the $\hat{\vartheta}_y$ rotation in this case being limited to ±15° with a 0.03° resolution. Three translation axes allow to change the position of the beam spot on the samples and to compensate for different sample thicknesses to achieve constant detection solid angle. Both sample holders are remotely operated by stepping motors that are fully computer controlled.

Both IBM and Cornell scattering geometries [19] can be used. However all the experiments described in this paper were performed with the IBM geometry and 170° scattering angle. Rectangular diaphragms of different widths at the chamber entrance and in front of the detectors allow high depth resolution grazing incidence and/or emergence experiments.

The active surface area of the detectors was either 25 or 50 mm^2, but the detector diaphragms defined a smaller area to achieve optimum energy resolution and detection efficiency. The pulses from the detector were amplified by commercial electronics and fed to the multichannel analyser. Energy spectrum distortion was minimised by pulse pile-up inspection and rejection with a time resolution better than 500 ns and by using count rates of no more than a few thousands of counts per second. Overall dead time correction was performed by counting, with fast electronics, all the pulses used to drive a Gated Biased Amplifier and the integral of the counts in the recorded spectrum.

The whole scattering chamber is fully isolated and acts as a Faraday cup. The overall precision in the beam current integration (by means of a commercial current integrator) is better than 0.5%. The RBS experiments are calibrated by using Ta/Si standard samples having an accuracy better than 2% [20].

In order to avoid channelling effects in single crystals the sample is rotated, while random spectra are recorded, in this way the beam describes a cone around a given axial direction, so that planar channelling effects are averaged. Actually, as actuating the motors induces eddy currents in the scattering chamber acting as a Faraday cup, the spectrum is obtained by the sum of many spectra recorded for small azimuthal angle increments. This is obtained by using both $\hat{\vartheta}_x$ and $\hat{\vartheta}_y$ tilt axes and the necessary computations of the $\hat{\vartheta}_x$ and $\hat{\vartheta}_y$ rotations are automatically performed by the computer control unit once the axial direction, the cone aperture angle, the azimuthal integral and step rotation angles have been assigned.

Random spectra are analysed by a computer simulation program where trial concentration profiles for the different elements are optimised until good agreement between the simulated and experimental spectra is found within the statistics.

For the C cross-section measurements a special target was prepared by the target service of LNL. A self-supporting C foil of nominal thickness 15 μg/cm^2 was first produced. On the two surfaces of the foil Au and Ag films were evaporated, nominally 50 and 100 nm thick respectively. The front Ag film is used as a spacer to separate the surface C contamination from the signal of the C foil and as a Rutherford reference element. The back Au film is used to prevent

systematic errors from the increasing C deposition during the measurements and as a second Rutherford reference element. The beam transmitted through the target hits a Be foil so that nearly no background counts are detected under the backscattering C signal.

In order to test the feasibility of C concentration measurements in Si targets, $Si_{1-x-y}Ge_xC_y/Si$ samples have been grown by MBE in a RIBER-SIVA 45 machine at the University of Linz. The growth temperature was fixed at 415°C and further details on sample growth are reported in Ref. [21]. A 50–100 nm Si cap layer was grown on top of the 250 nm thick alloy layer to separate the C signal of the surface contaminants from that of the alloy layer. The Ge composition has been determined by RBS [22] by using 2.0 or 3.0 MeV He beams, while the C concentration and lattice location have been measured by applying the technique described in the following.

Finally HRXRD rocking scans around the (0 0 4) Bragg reflection have been measured using a Philips HRD diffractometer equipped with a 4-crystal Ge (220) Bartels-type monochromator (primary beam divergence 12 arcsec). From these scans the lattice parameters in the growth direction have been determined.

3. Results and discussion

3.1. C cross-section

Fig. 1 shows the 5.750 MeV He backscattering spectrum of the Au/C/Ag target. The arrows indicate the scattering energies from the three elements at the surface. The surface C signal, due to the energy loss in the top Ag film, is sufficiently separated from the signal of the C foil so that its contribution to the C integral can be subtracted. In any case, it contributes a negligible amount (about 1%) to the whole C integral. Moreover the peaks of the three elements are each well separated and have a low background, whose shape is very regular. Background subtraction may thus be easily and accurately performed to obtain the net count integral, I, of each peak.

As a first approximation the peak integral of the top layer is related to the element areal density, N_s, by the relation

$$I = q\Omega\sigma(E_0)N_s \tag{1}$$

where q is the number of incident ions, Ω the detection solid angle and $\sigma(E_0)$ the cross-section of the given element at the incident energy E_0. A better approximation is obtained by introducing

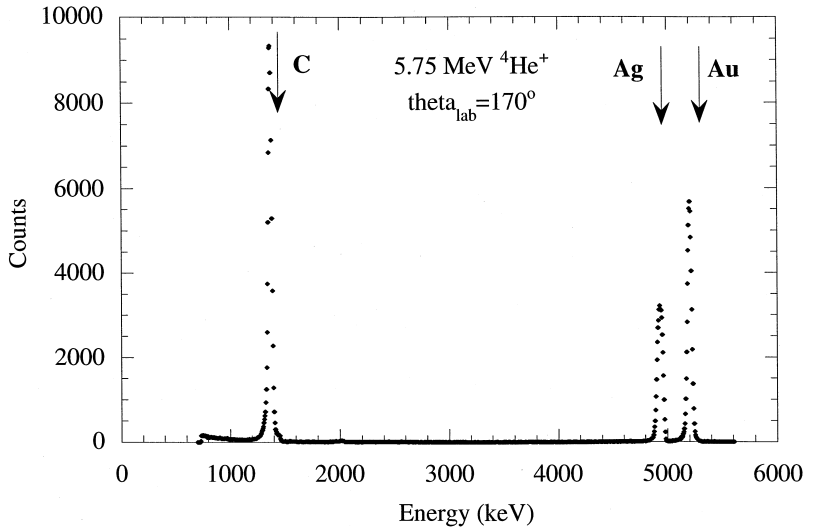

Fig. 1. 5.75 MeV He rBS spectrum of the Au/C/Ag calibration target.

correction terms to the cross-section to take into account the electron screening [23], f_s, to the Coulomb interaction of the incident ion of atomic number Z_1 with the nucleus of atomic number Z_2, and the variation of the cross-section due to the energy loss in the layer [19], $g(E_0, \Delta E_{in})$:

$$f_s = \left[\frac{1+\frac{1}{2}\frac{p}{E}}{1+\frac{p}{E}}\right]^2 \cong 1-\frac{p}{E}, \tag{2}$$

where E is the ion energy in the centre of mass reference system and $p = 0.049 Z_1 Z_2^{4/3}$ keV for a Thomas–Fermi screened potential [23]. In our range of energies and scattering angles this is an excellent approximation to the more accurate Dirac–Hartree–Fock–Slater description shown in Ref. [24]. The cross-section correction factor for the energy loss in the layer is given by

$$g(E_0, \Delta E_{in}) = \frac{E_0}{E_0 - \Delta E_{in}}, \tag{3}$$

where ΔE_{in} is the energy lost by the ion by traversing the layer in the way in.

In the case of non-Rutherford elastic scattering, the cross-section can be written as

$$\sigma(E) = R(E)\sigma_{Ruth}(E), \tag{4}$$

where $R(E)$ is the ratio of the actual to the Rutherford cross-section at any laboratory energy E.

Eqs. (1)–(3) can be easily extended to any layer of the stacked multilayer target. Then, provided the cross-section of Au and/or Ag is Rutherford, the cross-section ratio R is given by the expression

$$R(E) = \frac{I^C(E)}{I^{Au,Ag}(E)}\frac{\sigma_{Ruth}^{Au,Ag}}{\sigma_{Ruth}^{C}}\frac{f_s^{Au,Ag}(E)}{f_s^C(E)}\frac{g^{Au,Ag}(E)}{g^C(E)}\frac{N_s^{Au,Ag}}{N_s^C}. \tag{5}$$

It appears that to measure R the main needed quantity is the ratio of the heavy element to the carbon areal density. This quantity can be measured at a beam energy where both cross-sections are Rutherford. The C cross-section is known to be Rutherford at He beam energies lower than 2 MeV, so that at this energy $R = 1$ and the measured integrals can be used to derive the deviation from Rutherford at other energies

$$R(E) = \frac{I^C(E)}{I^{Au,Ag}(E)}\frac{I^{Au,Ag}(2)}{I^C(2)}\frac{f_s^{Au,Ag}(E)}{f_s^C(E)} \times \frac{f_s^C(2)}{f_s^{Au,Ag}(2)}\frac{g^{Au,Ag}(E)}{g^C(E)}\frac{g^C(2)}{g^{Au,Ag}(2)}. \tag{6}$$

This procedure is very accurate. In fact any error in the beam current integration and in the dead time correction is cancelled because only the ratio of the integrals is used. Moreover in Eq. (6) the integrals are measured quantities and only the correction factor ratios need to be computed. Their calculation involves the knowledge of the energy loss in each layer. To this purpose the areal densities obtained by calibrating the 2.0 MeV RBS experiment with the Ta/Si standard sample and the tabulated stopping powers [25] have been used. It is worth noting that any systematic error in the areal densities and/or in the stopping powers has nearly no influence on the final result for R. In fact the use of the ratio of the correction terms tends to cancel out the effect of these errors. The maximum error has been estimated by assuming a very large (10%) deviation in the stopping powers and it has been found to be much less than 1%. As a matter of fact the electron screening factor and the energy loss factor lead to a total correction to the integral ratios lower than 4%. Thus it can be concluded that the errors of this analysis method are essentially due to the counting statistics, systematic errors being virtually absent.

The measurements of the R deviation from Rutherford cross-section have been limited to the energy range 5.450–6.000 MeV which is the most useful for the application in an analytical technique as it will be shown later. The experimental results are given in Table 1 and in Fig. 2 were the data are reported at the mean energy in the C foil and not at the incident energy. Fig. 2 shows that the cross-section is constant (within the experimental errors of about 2.5%) at the level of 130 times Rutherford over the energy interval 5.67–5.75 MeV, allowing to analyse 640 nm of Si with high and constant sensitivity. Moreover in the energy interval 5.40–5.67 MeV the cross-section ratio varies slowly and almost linearly (about 0.15 keV^{-1}) allowing an easy integration of the cross-section correction in any analysis computer pro-

Table 1
Measured cross-section ratio $R(E) = \sigma/\sigma_{\text{Rutherford}}$ as a function of the average beam energy in the carbon foil

E (MeV)	$R(E)$
5.964	67.9
5.864	35.3
5.814	49.6
5.789	93.7
5.774	114
5.764	121
5.754	128
5.739	129
5.714	131
5.689	130
5.673	129
5.664	126
5.653	127
5.638	125
5.613	120
5.613	121
5.563	115
5.513	107
5.463	100
5.412	91.6

gram. This energy range corresponds to about 2 μm in the case of a silicon matrix.

The maximum sensitivity in C analysis by using this very broad resonance is almost the same as that of the 4.265 MeV resonance. The higher energy of the present resonance implies a lower stopping power and thus leads to a reduced depth resolution (in the case of Si the reduction is about 15%). This drawback is largely compensated by the advantages of the relative constancy of the cross-section. First of all the error introduced by an imperfect knowledge of the beam energy is very small. Of course it depends on the energy lost by the beam in the analysed layer: for a 0.5 μm Si layer a 10 keV error in the beam energy leads only to a 0.6% relative error in the average value of the cross-section. Moreover, the relative constancy of the cross-section over a large energy interval does not require to properly adjust the beam energy to the film thickness to achieve maximum sensitivity. As a consequence the measured C areal density is not severely affected by the used value of the stopping power and/or by the knowledge of the film thickness. Finally we want to underline that C lattice location by channelling analysis is nearly not affected by the reduced energy loss of the channelled beam (in axial channelling the energy loss is about 50–60% of the random energy loss). On the contrary by using the 4.265 MeV resonance this is a big problem because the measure of the interstitial or precipitated C fraction is related to

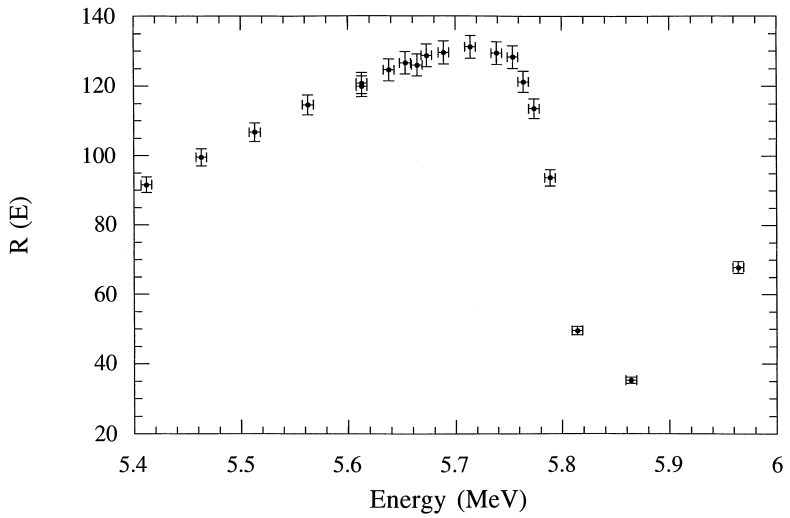

Fig. 2. Measured ratio of the C cross-section value with respect to the Rutherford one ($R(E)$), as a function of the mean energy in the C foil.

the C cross-section experienced by the channelled beam.

3.2. Conditions for the analysis of C in Si

The above characteristics suggest that this resonance in the elastic scattering cross-section is well adapted to C analysis. However C is normally contained in matrices heavier than C, so that its signal is superimposed on the background from the matrix. This fact determines the sensitivity limit of the analysis technique. However the main point here is that simple and accurate background subtraction is possible only if, in the energy region of the C signal, the background is a regular function of the energy. This could be a major problem in the case of Si whose cross-section is non-Rutherford above 3.8 MeV [26].

The 5.76 MeV He resonant backscattering (rBS) random spectrum of a Si sample is shown in Fig. 3. Many yield peaks can be observed. Apart from the surface C peak, the other peaks mimic the energy dependence of the Si cross-section resonances occurring at energies lower than the incident energy. In fact the beam loses energy by penetrating the Si target until the resonance energy is reached causing a yield enhancement. The energy lost by the scattered beam in the backward path to the detector determines the peak position in the spectrum while the observed peak width is mainly determined by the convolution of the resonance energy width and of the energy straggling (which is an increasing function of the traversed depth). For instance the surface peak in Fig. 3 is a residual of the resonance at 5.77 MeV, while the peaks at 3.14, 2.84 and 2.47 MeV correspond respectively to the 5.70, 5.56 and 5.37 MeV resonances occurring at 0.44, 1.49 and 2.75 μm below the surface.

Related to the C analysis the main problem appearing from Fig. 3 is the peak at about 1.3 MeV in the energy region below the signal of surface C. This peak corresponds to the 4.87 MeV resonance occurring at about 6 μm below the surface. To move the resonance peaks in the Si spectrum to other energy regions, a tilt angle in the IBM scattering geometry can be used. In this way the backward path of the scattered ions can be varied independently of the inward path which is fixed by the difference between the incident and the resonance energies.

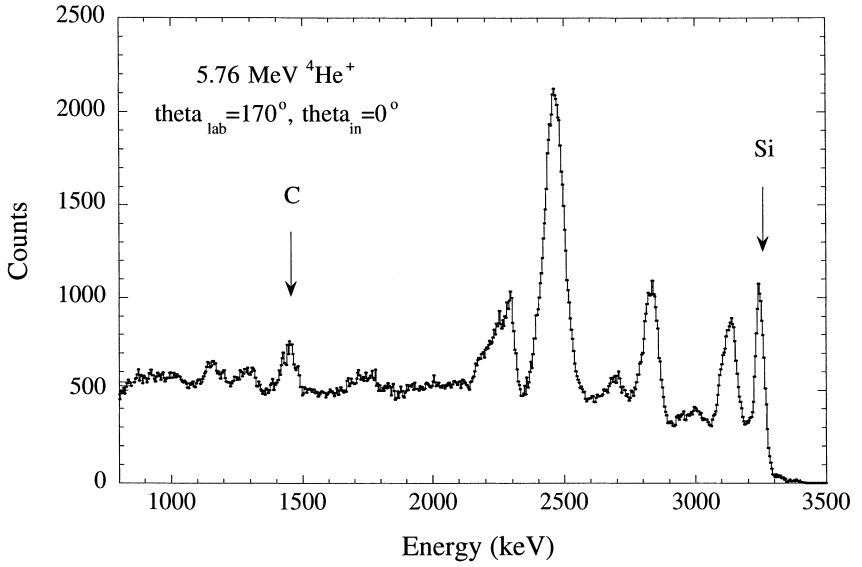

Fig. 3. 5.76 MeV rBS random spectrum of a Si sample. The experimental conditions are shown in the inset. The arrows represent the scattering energies from Si and C atoms at the surface.

This has been achieved, for instance, with a tilt angle of −60°, as illustrated in Fig. 4, for a beam energy of 5.75 MeV. As a matter of fact the resonance peaks are increasingly shifted to lower energies and broadened by increasing the depth where the resonance occurs. A magnification of the spectrum around the surface C energy is shown in Fig. 5(a). It appears that the background is reasonably regular. However a narrow peak is evident below the surface C peak. Although it has not been precisely identified its width suggests that it corresponds to a proton peak, most probably from the $^{28}Si(\alpha,p)^{31}P$ nuclear reaction. Its energy is weakly dependent on the beam energy and this feature can be exploited to avoid interference with the signal from buried C. By reducing the incident energy to 5.72 MeV the C surface peak is superposed to the proton peak as shown in Fig. 5(b).

To test the feasibility of C analysis under such condition, the amount of C surface contamination and its increase with the fluence has been studied and the results are shown in Fig. 6. The large intercept value is due to the fact that no special cleaning of the sample has been attempted before the analysis and to the integration of the proton peak in the C peak. The main result is thus the increase of the C dose with the beam charge showing that 0.067 C atoms/incident ion are deposited in our good vacuum conditions. For example, for a typical spectrum recorded with 150 μC on a beam spot area of 1 mm^2 an additional C surface contamination of about 6×10^{15} C/cm^2 must be expected. Thus reliable buried C analysis cannot be performed unless its signal is energy shifted with respect to the surface signal by means of a spacer (cap). In the case of Si, due to the used geometry, about 50 nm is sufficient.

3.3. Analysis of SiGeC samples

The analysis conditions found in the preceding section have been applied to the study of three $Si_{1-x-y}Ge_xC_y$ samples whose structure is given in Table 2. The samples have a nominal Ge composition as given by the growth parameters (column 2) whereas the C concentration (column 3) was determined by XRD before rBS analysis. The Ge fraction has been measured by using a 3 MeV He beam. A typical spectrum is shown in Fig. 7 together with the computer simulation obtained by neglecting the C fraction. The deduced Ge composition (x) value will be corrected after the C

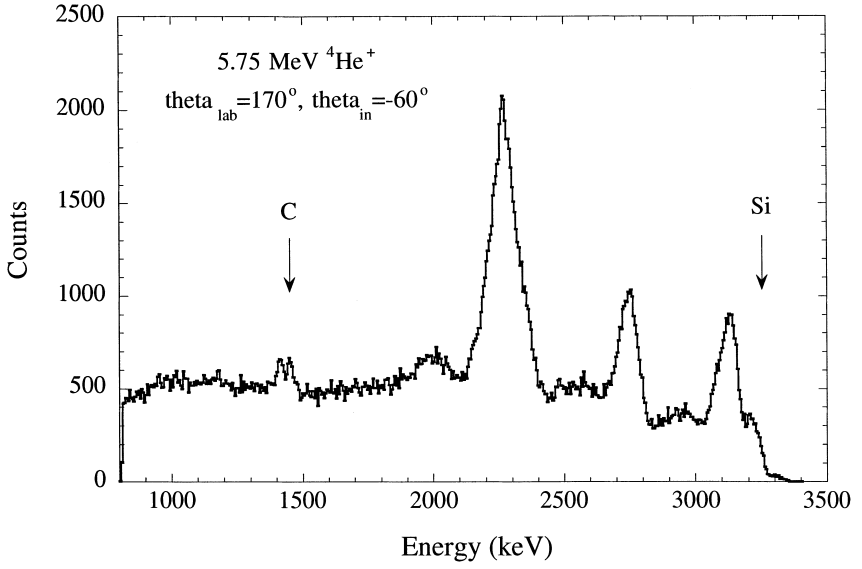

Fig. 4. 5.75 MeV rBS random spectrum of a Si sample. The experimental conditions are shown in the inset: IBM geometry, tilt angle $\theta_{in} = -60°$. Arrow meaning as in Fig. 3.

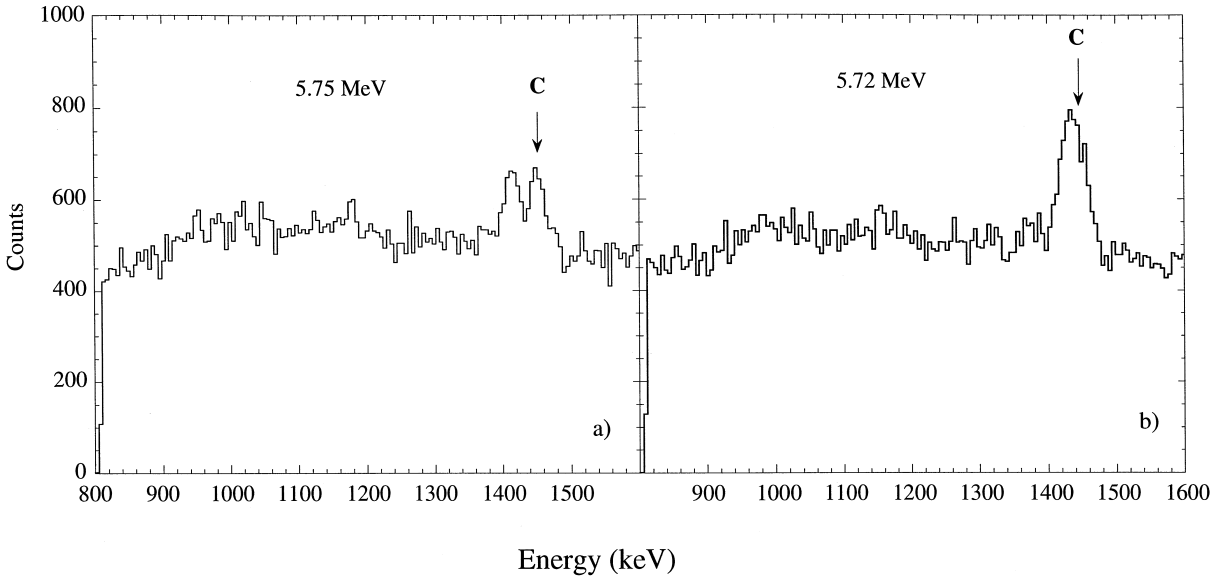

Fig. 5. Expanded view of the Si rBS spectra, recorded at $\theta_{in} = -60°$, for energies lower than 1.6 MeV: (a) 5.75 MeV $^4He^+$, (b) 5.72 MeV $^4He^+$.

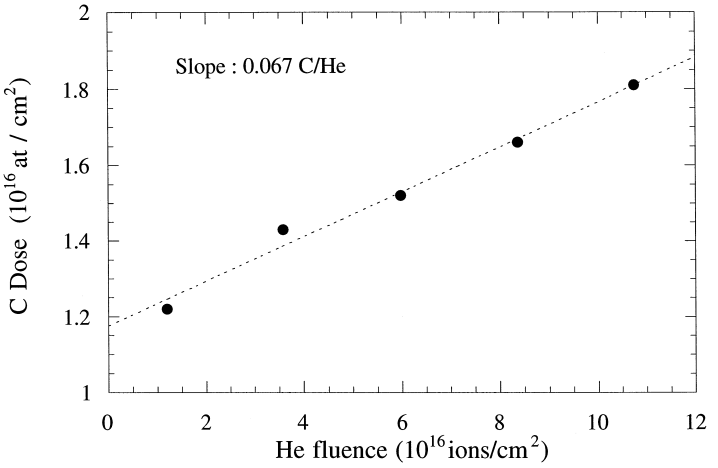

Fig. 6. C surface contamination as a function of the analysing beam fluence.

fraction has been found. The experimental values are given in column 4 of Table 2. The calibrated growth values do correspond to the measured ones within experimental error.

The rBS spectrum of the same sample obtained with a 5.72 MeV He beam is shown in Fig. 8 superposed on the corresponding spectrum of a Si sample. The Ge areal density, as determined from this spectrum, is the same as that determined from the 3 MeV spectrum indicating that the Ge cross-section is still Rutherford at this energy. An expanded view of the C energy region of the spectrum is shown in Fig. 9. The Si cap thickness (50 nm) is at the limit to produce a full energy

Table 2
The results of RBS and rBS analyses for three SiGeC samples are given in the last three columns. The second column gives the nominal growth values of the Ge concentration, while the third column gives the values of carbon concentration as determined by HRXRD

Sample	x_{nom} (at.%)	y_{XRD} (at.%)	x_{RBS} (at.%)	y_{rBS} (at.%)	Subs. fract.
254	15	1.73	15.1 ± 0.2	1.46 ± 0.03	0.79 ± 0.05
256	10	1.36	9.8 ± 0.5	0.97 ± 0.03	1.00 ± 0.08
257	10	1.18	10.0 ± 0.4	0.83 ± 0.03	1.00 ± 0.09

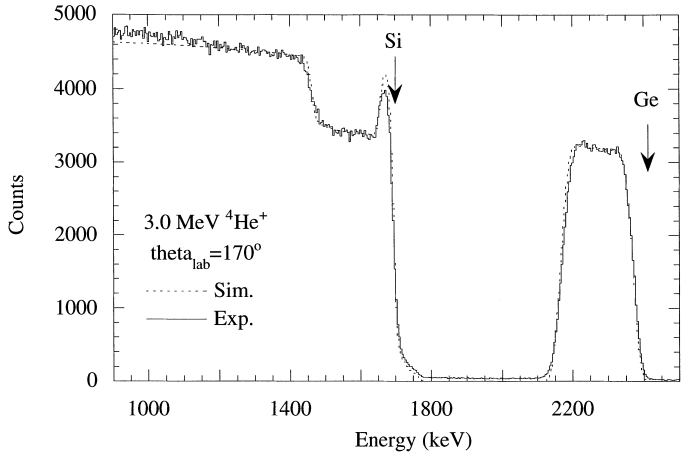

Fig. 7. 3 MeV RBS spectrum of the SiGeC sample #254. The dashed line is the RBS computer simulation of the spectrum. The arrows represent the scattering energies for Ge and Si atoms at the surface.

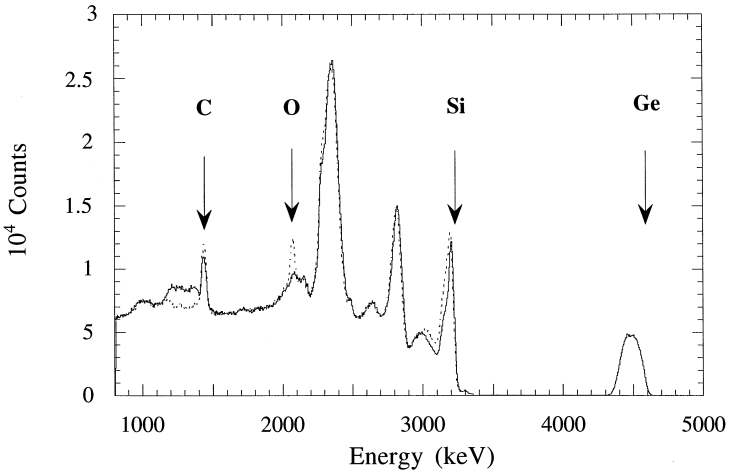

Fig. 8. rBS spectrum of sample #254 obtained with a 5.72 MeV He beam, superposed to the corresponding spectrum of a Si sample. The arrows represent the scattering energies for the labelled elements at the surface. The surface oxygen contamination is related to the Si sample.

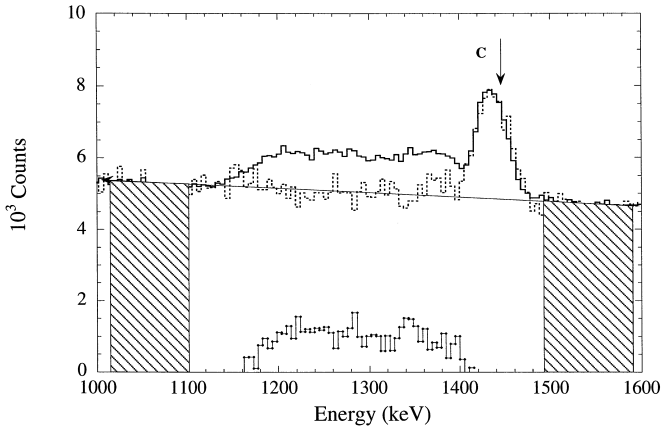

Fig. 9. Expanded view of the C energy region of the spectra in Fig. 8. The dashed areas show the energy windows used for automatic Si background subtraction in recording C channelling dips. The line represents the resulting interpolated background. In the bottom part of the figure the subtracted C signal of the SiGeC film is also reported.

separation from the C surface peak. Nevertheless, by subtracting the Si background spectrum, the C signal from the SiGeC film (bottom part of Fig. 9) is well resolved. By assuming a constant C concentration profile, the average C concentration can be obtained from the ratio of the C and Ge peak integrals taking into account the respective cross-sections. Alternatively, the C concentration can be measured by the height of the C signal. Both analysis procedures produced the same C concentration values, within the experimental uncertainty of the procedures. The results are given in the fifth column of Table 2. A large, systematic discrepancy with the HRXRD data is evident.

The resonance at 5.72 MeV with the described experimental set-up allows also lattice location measurements in channelling configuration. Angular scans across the [1 1 1] axis permit to evaluate the substitutional fraction of carbon by comparing minimum yield, χ, and channelling dip shape of the carbon signal to those of silicon.

The C channelling dip cannot be obtained in the usual way, i.e. by simply selecting an energy window in the spectrum, because of the large Si background. Thanks to the selected measuring conditions the Si background in the C region is quite smooth (see Fig. 9) and it can be roughly approximated by a straight line. This fact allows an automatic background subtraction by selecting two additional energy windows above and below the C region, as shown in Fig. 9. The $\langle 1\ 1\ 1 \rangle$ channelling dips of samples 257 and 254, recorded in this way, are shown in Fig. 10(a) and (b), respectively. Of course the reported Si signal corresponds to Si in the SiGeC film.

A more accurate background subtraction can be made by recording the spectra relative to selected angular positions in the angular scans both for the sample and for a Si crystal (background subtraction reference sample). In order to achieve good statistics this procedure requires a considerable ion beam fluence so that ion beam induced damage must be expected. To this end the beam induced damage was also investigated and the results will be reported elsewhere. Suitable conditions, leading to constant substitutional fractions after repeated measurements on the same spot, were found with a relatively large beam cross-section (2×1 mm^2) and detection solid angle (6 msr).

For samples #256 and #257 (Fig. 10(a)) the C and Si dips are identical within the error bars indicating a complete carbon substitutionality. For sample #254 (Fig. 10(b)) the C dip has the same width as the Si dip but the minimum yield is significantly higher indicating that C is only partially substitutional. In this case the substitutional C fraction turns out to be $f = 0.79 \pm 0.05$. The Ge

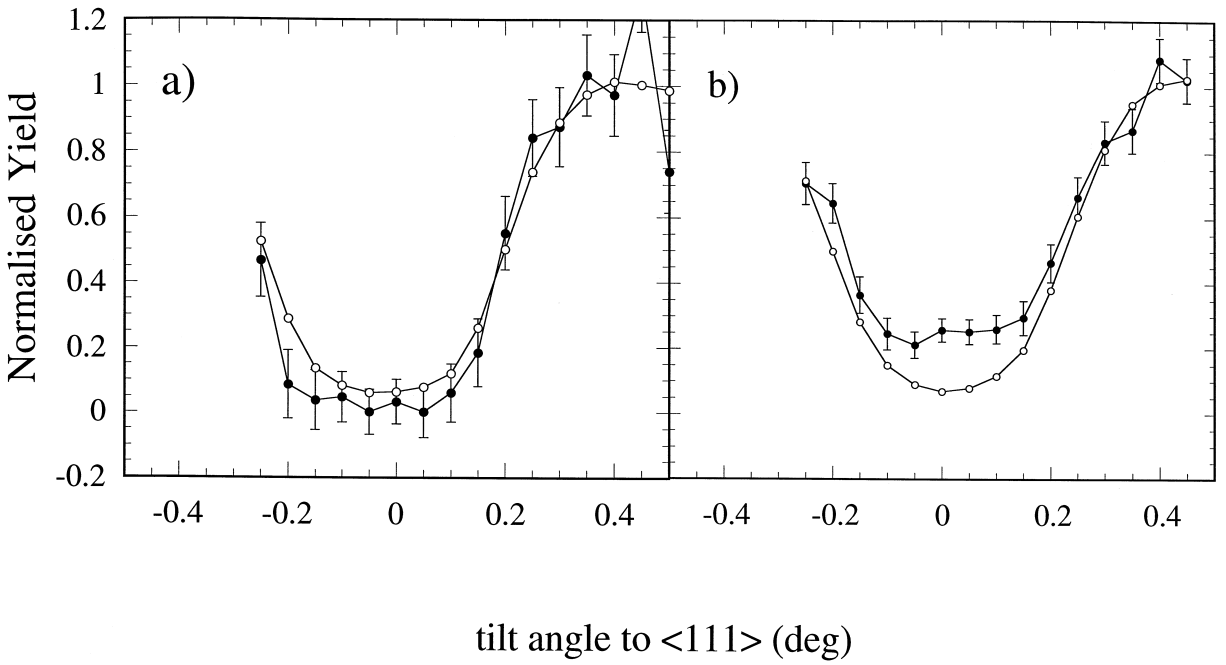

Fig. 10. C and Si channelling dips across the [1 1 1] axis of samples #257 (a) and #254 (b). The Si and C yields are normalised to their random levels. Open circles: Si yield; full circles: C yield.

channelling dips were also recorded for all samples and showed that Ge is substitutional in the Si lattice.

The C composition data given in Table 2 show that HRXRD data are systematically higher than rBS data, the discrepancy being well above the combined error of the two measurements. In this respect it must be stressed that the rBS measure is a direct determination while HRXRD measures the lattice parameter which is converted to element concentrations mainly through the assumption that alloy lattice parameters follow the Vegard's rule.

The data for C concentration by HRXRD in Table 2 were obtained by taking into account the non-linear behaviour of the lattice constant with composition of the Si–Ge system [15] and by assuming Vegard's rule to hold for the Si–C system (from Si to diamond). The comparison of the C concentration data in Table 2 suggests a large deviation from Vegard's rule for the Si–Ge–C system in the same direction found theoretically by Kelires [17] for the Si–C system. A more systematic investigation of this problem will be the object of a forthcoming report.

4. Conclusions

We have shown that $^{12}C(\alpha,\alpha)^{12}C$ resonant backscattering at 5.7 MeV can be used to analyse C in silicon based heterostructures. Layers with thicknesses up to 640 nm can be analysed with a nearly constant (within 5%) cross-section about 130 times higher than the corresponding Rutherford value. This allows to detect carbon concentrations of about 1 at.% with an absolute error of 0.03 at.% Moreover the use of this resonance is not strongly affected by channelling energy loss which leads to accurate C substitutional fractions.

Both these characteristics make the 5.7 MeV resonance more adapted to the analysis of C in SiGeC and SiC alloys than the previously used 4.265 MeV resonance. Preliminary results suggest a strong deviation from Vegard's rule for the SiGeC system.

Acknowledgements

This work has been partly supported by INFM PRO-FESR-RIM. The authors are indebted to G. Manente for the preparation of the Au/C/Ag targets and to I. Motti for the assistance during the measurements.

References

[1] S. Furukawa, H. Etoh, A. Ishizaka, T. Shimada, Semiconductor with crystalline silicon–germanium–carbon alloy, US Patent #4.885.614, Dec 5, 1989.
[2] H.J. Osten, E. Bugiel, P. Zaumseil, Appl. Phys. Lett 64 (1994) 3440.
[3] G. Davies, R.C. Newman, in: T.S. Moss (Ed.), Handbook of Semiconductors, vol. 3, Elsevier Science, New York, 1994.
[4] K. Eberl, S.S. Iyer, J.C. Tsang, M.S. Goorsky, F.K. LeGoues, J. Vac. Sci. Tech. B 10 (1992) 934.
[5] K. Eberl, S.S. Iyer, S. Zollner, J.C. Tsang, F.K. LeGoues, Appl. Phys. Lett 60 (1992) 3033.
[6] J.W. Strane, H.J. Stein, S.R. Lee, S.T. Picraux, J.K. Watanabe, J.W. Mayer, J. Appl. Phys. 76 (1994) 3656.
[7] R.G. Wilson, F.A. Stevie, Ch.W. Magee, Secondary Ion Mass Spectrometry, Wiley, New York, 1989.
[8] M. Östling, C.S. Petersson, G. Possnert, Nucl. Instr. and Meth. 218 (1983) 439.
[9] J.A. Leavitt, L.C. McIntyre, Jr., P. Stoss, J.G. Oder, M.D. Ashbaugh, B. Dezfouly-Arjomandy, Z.M. Yang, Z. Lin, Nucl. Instr. and Meth. B 40–41 (1989) 776.
[10] Y. Feng, Z. Zhou, Y. Zhou, G. Zhao, Nucl. Instr. and Meth. B 86 (1994) 225.
[11] J.A. Leavitt, L.C. McIntyre, Jr., M.D. Ashbaugh, R.P. Cox, Z. Lin, R.B. Gregory, Nucl. Instr. and Meth. B 118 (1996) 613.
[12] A.E. Bair, Z. Atzmon, S.W. Russel, J.C. Barbour, T.L. Alford, J.W. Mayer, Nucl. Instr. and Meth. B 118 (1996) 274.
[13] B. Maurel, G. Amsel, J.P. Nadai, Nucl. Instr. and Meth. 197 (1982) 1.
[14] L. Vegard, Z. Phys. 5 (1921) 17.
[15] J.P. Dismukes, L. Ekstrom, R.J. Paff, J. Phys. Chem. 68 (1964) 3021.
[16] M. Melendez-Lira, J. Menendez, W. Windl, O.F. Sankey, G.S. Spencer, S. Sego, R.B. Culbertson, A.E. Bair, T.L. Alford, Phys. Rev. B 54 (1996) 12866.
[17] P.C. Kelires, Phys. Rev. B 55 (1997) 8784.
[18] S. Hao, C.H. Sheng, T. Jia-yong, Y. Fujia, Acta Phys. Sinica 43 (1994) 1569.
[19] J.R. Tesmer, M. Nastasi (Eds.), Handbook of Modern Ion Beam Materials Analysis, Materials Research Society, Pittsburgh USA, 1995.
[20] C. Cohen, J.A. Davies, A.V. Drigo, T.E. Jackman, Nucl. Instr. and Meth. 218 (1983) 147.
[21] S. Zerlauth, C. Penn, H. Seyringer, F. Schäffler, Appl. Phys. Lett. 72 (13) (1998) 1602.
[22] A. Armigliato, M. Servidori, F. Cembali, R. Fabbri, R. Rosa, F. Corticelli, D. Govoni, A.V. Drigo, M. Mazzer, F. Romanato, S. Frabboni, R. Balboni, S.S. Iyer, A. Guerrieri, Microsc. Microanal. Microstruct. 3 (1992) 363.
[23] J. L'Ecuyer, J.A. Davies, N. Matsunami, Nucl. Instr. and Meth. 160 (1979) 337.
[24] H.H. Andersen, F. Besenbacher, P. Loftager, W. Möller, Phys. Rev A 21 (1980) 1891.
[25] J.F. Ziegler, Stopping Power and Ranges of Ions in Matter, vol. 4, Pergamon Press, New York, 1977.
[26] C.H. Sheng, S. Hao, Y. Fujia, T. Jia-yong, Nucl. Instr. and Meth. B 85 (1994) 47.